Report

Current Biology

Fear-Related Signals in the Primary Visual Cortex

Highlights

- Responses of neurons in monkey V1 are rapidly modified by visual fear conditioning
- Fear-related signals in V1 emerge from the outset of neuronal responses (<40 ms)
- Fear learning in V1 is specific to the CS orientation and location
- The conditioning effect is independent of neurons' orientation preferences

Authors

Zhihan Li, An Yan, Kun Guo, Wu Li

Correspondence

liwu@bnu.edu.cn

In Brief

By pairing grating patterns with aversive stimuli, Li et al. show fear-induced changes in monkey V1. Fear-related signals in V1 arise from neuronal response outset (<40 ms) and are present even if the gratings are rendered invisible, suggesting a bottom-up mechanism for proactive tagging of visual inputs that are predictive of imminent threat.

Li et al., 2019, Current Biology *29*, 4078–4083
December 2, 2019
https://doi.org/10.1016/j.cub.2019.09.063

CellPress

CellPress

Current Biology
Report

Fear-Related Signals in the Primary Visual Cortex

Zhihan Li,[1] An Yan,[1] Kun Guo,[2] and Wu Li[1,3,*]
[1]State Key Laboratory of Cognitive Neuroscience and Learning and IDG/McGovern Institute for Brain Research, Beijing Normal University, Beijing 100875, China
[2]School of Psychology, University of Lincoln, Lincoln LN6 7TS, UK
[3]Lead Contact
*Correspondence: liwu@bnu.edu.cn
https://doi.org/10.1016/j.cub.2019.09.063

SUMMARY

Neuronal responses in the primary visual cortex (V1) are driven by simple stimuli, but these stimulus-evoked responses can be markedly modulated by non-sensory factors, such as attention and reward [1], and shaped by perceptual training [2]. In real-life situations, neutral visual stimuli can become emotionally tagged by experience, resulting in altered perceptual abilities to detect and discriminate these stimuli [3–5]. Human imaging [4] and electroencephalography (EEG) studies [6–9] have shown that visual fear learning (the acquisition of aversive emotion associated with a visual stimulus) affects the activities in visual cortical areas as early as in V1. However, it remains elusive as to whether the fear-related activities seen in the early visual cortex have to do with feedback influences from other cortical areas; it is also unclear whether and how the response properties of V1 cells are modified during the fear learning. In the current study, we addressed these issues by recording from V1 of awake monkeys implanted with an array of microelectrodes. We found that responses of V1 neurons were rapidly modified when a given orientation of grating stimulus was repeatedly associated with an aversive stimulus. The output visual signals from V1 cells conveyed, from their response outset, fear-related signals that were specific to the fear-associated grating orientation and visual-field location. The specific fear signals were independent of neurons' orientation preferences and were present even though the fear-associated stimuli were rendered invisible. Our findings suggest a bottom-up mechanism that allows for proactive labeling of visual inputs that are predictive of imminent danger.

RESULTS

Fear-Related Signals in V1

We adapted the fear-conditioning paradigm from a previous study [10]. Within a block of trials (Figure 1A), an aversive air puff delivered to the face was used as the unconditioned stimulus (US). Drifting square-wave gratings tilted to one side from the vertical (e.g., rightward 15°, 45°, or 75° with equal probability) served as the conditioned stimuli (CSs) and were paired with the air puff. Gratings tilted to the opposite side (e.g., leftward 15°, 45°, or 75°) served as the control stimuli (referred to as the non-conditioned stimuli [NSs]) and were paired with a juice reward. The two groups of CSs and NSs were randomly interleaved at a ratio of 1:3 within the same block of trials (30 CSs and 90 NSs). While the monkey was fixating on a small spot, V1 responses to the gratings (400 ms exposure) were recorded with implanted microelectrode arrays. Before the delivery of the air puff in the CS trials or the juice reward in the NS trials, a blank-screen interval (500 ms, termed the trace interval) was used for monitoring the animal's eye-blink response as an assessment of fear-associated behavior. The inter-trial interval was 2–3 s.

Keeping the CS and NS orientations unchanged, we conducted the experiment for 4 and 6 days on monkey MA (5–10 blocks of trials per day) and MB (8–13 blocks per day), respectively. Afterward, we switched the CS and NS orientations (previous CS became NS and vice versa) and continued the experiment for another 9 and 4 days on MA and MB, respectively. Before and after the conditioning on each day, we recorded V1 responses to the gratings in the absence of the air puff. The pre-conditioning test was taken as a baseline control for the effects of conditioning on neuronal responses; the post-conditioning test was used for fear extinction. The pre- and post-tests contained 2 or 3 blocks of trials; each block comprised 10 randomized repetitions of each grating orientation.

To assess fear-associated behavior, we separated the CS and NS trials (Figures 1B and S1A). Only in the CS trials did the animals show striking eye-blink responses in the trace interval before the air puff.

To evaluate fear-related V1 responses, we treated data collected by the same electrode across different days as coming from the same V1 site. The data were pooled and averaged across days for each site before we averaged over the population; the Wilcoxon signed-rank test was used for all statistical comparisons unless otherwise stated.

We first compared the mean neuronal responses evoked by the CS and NS gratings in the conditioning sessions with those in the pre-tests (Figure 1C, population responses; Figure S2A, examples of V1 sites). Conditioning resulted in a slight elevation of the spontaneous activity before the onset of gratings (an increase of 2.7 ± 0.4 Hz relative to the pre-test level of 9.7 ± 0.9 Hz, mean ± SEM, n = 90 V1 sites by pooling data in Figure 1C). After discounting this general arousal effect, we observed an additional enhancement (defined as the fear-related signal) in

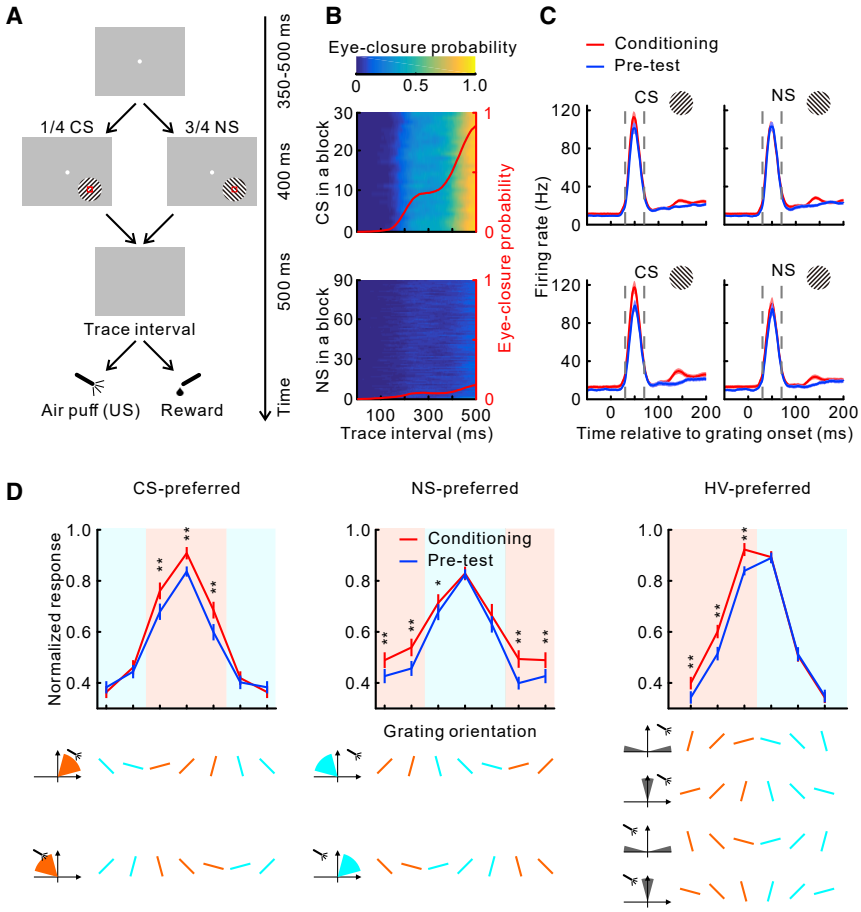

Figure 1. Fear-Related Signals in V1

(A) Time course of the conditioning trials. The CS and NS gratings (4° in diameter) were centered on V1 receptive fields (RFs; each red square illustrates one recording site).

(B) Eye-blink responses within the trace interval. Two monkeys (MA and MB) learned to reflexively blink in anticipation of the air puff associated with the CS (top), in contrast to the NS (bottom). We calculated eye-closure probabilities (color coded) in 2 ms bins for each trial in a block by averaging over 205 blocks of trials pooled from both animals. Curves show the mean probability averaged across all CS or NS trials.

(C) Mean V1 responses (1 ms bins smoothed by 10 ms moving window) in the conditioning sessions (red) and pre-tests (blue) for the CS (left) and NS (right). Two rows correspond to two opposite CS and NS configurations (see insets; upper row: n = 88 V1 sites, including 47 and 41 from MA and MB, respectively; lower row: n = 81, including 40 and 41 from MA and MB, respectively). Vertical dashed lines specify the time window (30–70 ms) used for quantifying the fear-related signals. Shadowing shows mean ± SEM.

(D) Conditioning effects on orientation tuning functions. V1 sites were separated into 3 groups: the CS-preferred (n = 68, including 38 and 30 from MA and MB, respectively), NS-preferred (n = 68, including 36 and 32 from MA and MB, respectively), and HV-preferred (n = 48, including 29 and 19 from MA and MB, respectively). Bottom insets illustrate the ranges of the preferred orientations for each group of V1 sites (color sectors; the two opposite CS and NS configurations shown in C are pooled) and the orientations of gratings (color bars: orange, CS; cyan, NS). The averaged tuning curves in the conditioning sessions (red) and pre-tests (blue) were constructed with neuronal responses within 30–70 ms as a function of the grating orientations denoted in the insets. The tuning curves from individual V1 sites were normalized so that the tuning peak in the pre-test was unity for each site. Error bars represent mean ± SEM. *$p < 0.05$; **$p < 10^{-3}$.

See also Figures S1 and S2.

the early phase of V1 responses to the CS (a relative increase of 14.8% ± 1.6%, mean ± SEM, within 30–70 ms, $p < 10^{-11}$), in contrast to the NS (1.8% ± 1.3%, $p = 0.34$). The fear-related signals associated with the CS were significant in the majority of recorded V1 sites (66/90, 73%; Mann-Whitney U test, $p < 0.05$). The estimated latency of these signals (35.3 ± 1.0 ms, mean ± SD calculated by resampling of all sites; see STAR Methods) was comparable to V1 response latencies to the CS (35.9 ± 0.8 ms) and NS (35.3 ± 0.9 ms). These results indicate that V1 neurons convey specific fear-related signals from their response outset.

To further isolate the fear-related signals specific to the CS and also to eliminate a potential confounding factor caused by a general drift of neuronal firing rates in the conditioning session relative to the pre-test, we subtracted the fear-related signals associated with the NS from those associated with the CS (defined as the differential fear signals). The differential fear signals were comparable between the two animals in magnitude (MA: 12.0% ± 1.1%, mean ± SEM, $p < 10^{-8}$; MB: 14.3% ± 2.0%, $p < 10^{-7}$) and latency (MA: 38.6 ± 0.8 ms, mean ± SD; MB: 43.9 ± 2.7 ms; Figure S2B); they were not caused by differential visual adaptation of neuronal responses to the CS and NS gratings that were displayed at an unequal frequency of 1:3 (Figure S2C).

Besides the early fear-related responses, a late enhancement (>100 ms after the onset of gratings) was seen in both the CS and NS trials (Figure 1C). This late and nonspecific component, which was observed only in MB (Figure S1B), might have been caused by spatial attention to the gratings during the conditioning.

Given that V1 neurons often show orientation selectivity, we examined whether the early fear-related signals were dependent on neurons' orientation tuning. Given that the gratings were left or right tilted by 15°, 45°, or 75°, we divided the orientation space (0°–180°) into three equally sized compartments: 45° ± 30° (right tilted), 135° ± 30° (left tilted), and 90° ± 15° combined with 0° ± 15° (near vertical and near horizontal). The V1 sites were first assigned to these compartments according to their preferred orientations and were then classified into three groups relative to the CS and NS orientations (Figure 1D): the CS-preferred, NS-preferred, or horizontal- and vertical-preferred (HV-preferred) sites with orientation tuning peaks distributed, respectively, around the CS, NS, or vertical and horizontal orientations.

For each group of V1 sites pooled from both animals and from two opposite CS and NS configurations (right- and left-tilted CS;

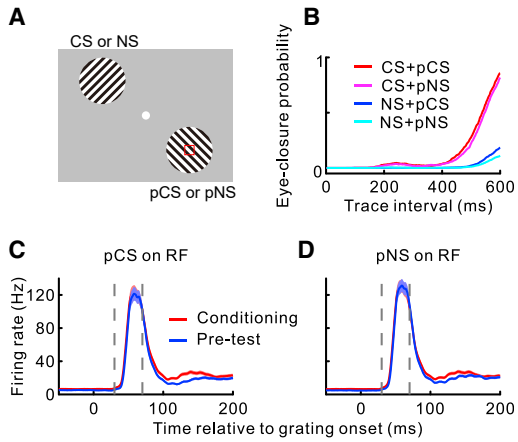

Figure 2. Location Specificity of the Conditioning Effect

(A) Sample stimuli. Only 45° and 135° gratings were used in this experiment. Fear conditioning was first established at the location where the CS and NS were presented. The second grating patch (probe stimulus, pCS or pNS) was then introduced to probe V1 responses. The red square illustrates the RF of a recording site.

(B) Mean eye-blink responses during the trace interval for the four combinations of CS or NS and pCS or pNS. Data were averaged across 83 blocks of trials (20 CSs and 60 NSs per block) tested on monkey MB over 4 days.

(C and D) Mean V1 responses to the probe gratings that coincided with the CS (C) or NS (D) orientation in the conditioning sessions (red) and pre-tests (blue). Vertical dashed lines mark the 30–70 ms window for calculating the fear-related signals (not statistically significant: p = 0.27 in C, p = 0.36 in D; n = 56 V1 sites). Shadowing shows mean ± SEM.

Figure 1D insets), we compared the averaged orientation tuning curves in the conditioning sessions and pre-tests. Fear-induced enhancement in V1 early response was observed in all three groups of V1 sites around the CS orientations, leading to changes in their tuning curves in different manners (Figure 1D): a heightened peak and thus a larger amplitude of the tuning curve for the CS-preferred sites, elevated flanks and thus a smaller amplitude of the tuning curve for the NS-preferred sites, and an asymmetric elevation of the tuning curve for the HV-preferred sites. These changes were largely consistent between the two animals (Figure S1C).

Although the CS-specific conditioning effect was independent of neurons' orientation preferences, it was confined to the visual-field location where the CS was presented. After the fear conditioning was well established in monkey MB by presenting the CS and NS in the visual-field quadrant opposite to the recorded receptive fields (RFs), a second grating patch was introduced to probe neuronal responses (Figure 2A). The probe stimulus was centered on the RFs and was randomly set at the CS or NS orientation. During the trace interval, the fear-associated eye-blink responses were largely linked to the CS at the conditioned location, regardless of the orientations of the probe gratings (Figure 2B). Correspondingly, the fear-related signals were absent during the initial phase of neuronal responses in V1 at the retinotopic location of the probe gratings (Figures 2C and 2D).

Fear-Related Signals in V1 to Invisible Gratings

The early emergence of fear-related signals in V1 with latencies comparable to visually evoked responses suggests a fast bottom-up process rather than reentrant feedback modulation. This conjecture was supported by another experiment on monkey MB: the fear-related V1 signals were still present even though the CS and NS orientations were masked by the addition of horizontally oriented drifting gratings. The subjective percept of such compound stimuli became moving plaids rather than the component gratings of clearly visible CS or NS orientations (Figure 3A). During the conditioning (as in Figure 1A), we randomly replaced 20% of the CS and NS gratings with the corresponding plaids, which were not paired with an air puff. Behaviorally (Figure 3B), the eye-blink responses were neglectable and indistinguishable among the NS gratings and the two types of plaids. However, the plaids containing the CS component activated significant early fear-related signals in V1 (15.0% ± 2.7%, mean ± SEM, n = 49, $p < 10^{-8}$; Figure 3C upper right), and these signals are comparable to those activated by the CS gratings (16.2% ± 2.0%; Figure 3C upper left), but the signals were nearly absent for the plaids containing the NS component (2.7% ± 1.4%, p = 0.08; Figure 3C lower right).

Time Course of Fear Learning in V1

To examine the time course of the formation and extinction of the fear-related signals in V1, we separated—for the data shown in Figure 1C—the first and last blocks of daily conditioning trials from intermediate blocks and compared them with the pre- and post-tests. In the pre-test, the difference of mean V1 responses to the CS and NS was negligible (Figure 4A, the first pair of data points; see also Figure S4A for data separated for each animal). In the conditioning session, the fear-related signals emerged in the first block of trials, where signals at the CS were stronger than those at the NS orientations (Figures 4A and 4B; see Figure S4 for results from each animal). The mean neuronal firing rates tended to decline with further conditioning (Figure 4A; more evident in monkey MA, Figure S4A), but the differential fear signals (CS-NS difference) were retained or even enlarged (Figures 4A and 4B; see also Figures S4A and S4B). In the post-test when the air puff was removed, the CS-NS difference was rapidly diminished.

To further examine the dynamic and specific changes in V1 over the course of fear learning, we trained monkey MB by double reversal (back-and-forth switching) of the CS and NS orientations within a single day. Each block of trials was reduced by half (15 CSs and 45 NSs per block). After each reversal (Figure 4C), the fear-related signals associated with the previous CS (new NS) rapidly diminished in the first block of trials and were abolished in the second block. In the meantime, the fear-related signals emerged at the new CS orientations and rapidly plateaued after ~3 blocks of trials. Replotting data according to the sequence of individual CS presentations (see Figure S4C) showed that after each reversal the new CS induced significantly larger fear-related signals than the new NS after ~15 presentations of the CS and that in the post-test, the CS-NS difference remained statistically significant until ~20 presentations of the CS gratings (i.e., two blocks of post-test trials).

DISCUSSION

The current study showed that V1 neuronal responses were rapidly modified by a small number of CS-US associations.

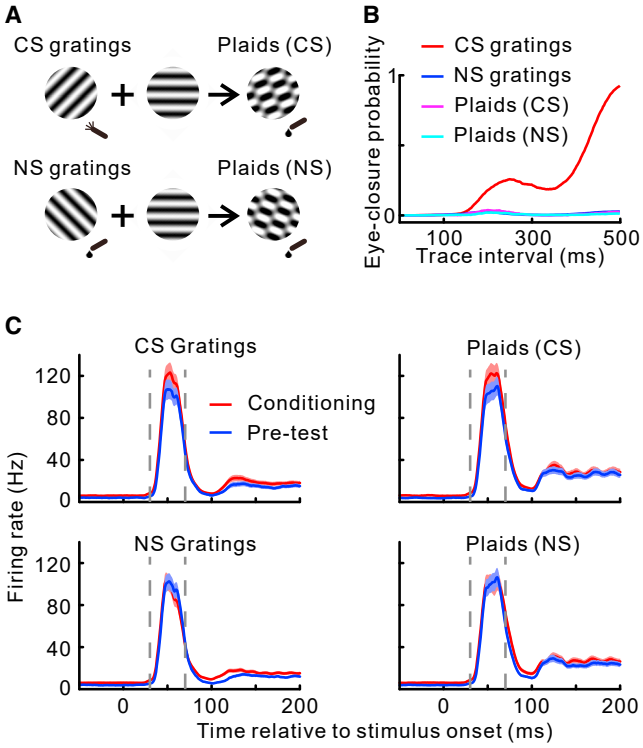

Figure 3. Fear-Related Signals in V1 to Invisible Gratings

(A) Moving plaids formed by superposition of the CS or NS (sinusoidal drifting gratings) with drifting horizontal gratings. In this experiment, only 45° and 135° gratings were used as the CS or NS.

(B) Mean eye-blink responses in the trace interval for the four types of stimuli mixed within the same block of trials (24 and 72 trials for the CS and NS gratings, respectively, and 6 and 18 trials for the plaids containing the CSs and NSs, respectively). Data were averaged across 120 blocks of trials tested on MB over 12 days and balanced with two opposite CS and NS configurations.

(C) Mean V1 responses (n = 49) to the four types of stimuli in the conditioning sessions (red) and pre-tests (blue). Vertical dashed lines mark the 30–70 ms window for calculating the fear-related signals. Shadowing shows mean ± SEM.

See also Figure S3 for examples of individual V1 sites.

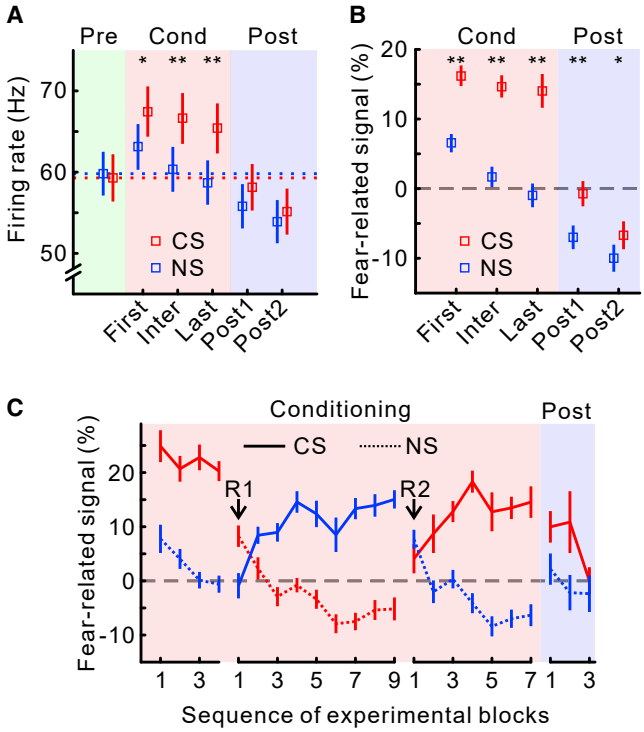

Figure 4. Time Course of Fear Learning in V1

(A) The mean population firing rates (30–70 ms after CS or NS onset with spontaneous activity subtracted) were separated for the specified blocks of trials (same data as in Figure 1C with two opposite CS and NS configurations pooled; n = 90 from MA and MB). The background colors delimit the data from the pre-test, the conditioning session (first block, intermediate blocks, and last block), and the post-test (two separate blocks). The number of intermediate conditioning blocks were between 3 and 11 in different days.

(B) Same data in (A) are replotted and show the mean fear-related signals: percent changes in mean firing rate relative to the pre-test rate were calculated for individual V1 sites and then averaged.

(C) Fear-related signals in V1 during double reverse learning within a single day (n = 62 V1 sites from MB). Data were pooled from repeated experiments over 11 days. In the first 6 days, daily conditioning began with 135° CS (45° NS) and ended with the same CS and NS orientations after the two reversals (R1 and R2). In the remaining 5 days, daily conditioning started with 45° CS (135° NS). Each conditioning block comprised 15 CS and 45 NS trials. Post-test results are also shown.

All error bars represent mean ± SEM. *$p < 0.05$, **$p < 10^{-3}$ for the difference between the CS and NS. See also Figure S4 for replotted (A) and (B) with data separated between the two animals and for replotted (C) according to the sequence of individual CS presentations.

The fear-induced changes in V1 were seen from neuronal response outset and were restricted to the CS orientation and location. Together with the observation that the fear-related V1 signals were still present after the CS orientation was rendered invisible, our findings suggest the formation of implicit fear memory in V1, which allows for proactive tagging of visual inputs that are predictive of imminent danger.

It has been shown that neuronal responses in monkey V1 can be modulated by non-sensory factors such as attention and reward [11, 12]. These modulatory effects are present only in the late components of V1 responses (>100 ms after the onset of a visual stimulus), indicating feedback neural processes. In contrast, the fear-related signals emerged in the early components (30–70 ms) of V1 responses, which are also several tens of milliseconds earlier than the reported latencies of amygdala neurons in response to visual inputs [10, 13–16]. The early emergence of fear-related signals in V1 excludes the possibility that they are simply a signature, on a trial-by-trial basis, of feedback modulations from the amygdala or other areas.

Monkey physiological studies on perceptual learning have shown that response properties of V1 neurons can be altered by extended training on a visual task [17–19]. It has been proposed that cortical plasticity induced by perceptual learning is guided by two types of modulatory signals [20]: (1) reward-related diffusive neuromodulatory signals (e.g., from the dopamine and acetylcholine systems) that are responsible for synaptic changes and (2) top-down selection signals for restricting the changes among the most informative neurons representing behavior-relevant information. The V1 changes induced by fear conditioning could be implemented in an analogous manner, except that the fear signals generated by the amygdala

could serve as a more potent reinforcer to drive the cortical changes.

The amygdala, which is indispensable in fear learning [21], is directly connected with visual areas, including V1, forming a closed loop [22, 23]. Another structure, the pulvinar, is intimately connected with the visual areas and amygdala: these brain structures together constitute intricate networks for coordinating sensory and emotional processing [24, 25]. It has been shown that, rather than simply exerting delayed feedback modulation on a trial-by-trial basis, the pulvinar plays an important role in coordinating visual processing by gating the feedforward processes or maintaining a certain cortical state. Such a gating mechanism can profoundly affect the early phasic-output signals from visual areas [26, 27]. We speculate that, in fear learning, the amygdala might either play a similar gating role or interact with the pulvinar's gating process through its direct projections to V1 superficial layers [23]. With a few CS-US associations during the initial conditioning, the intrinsic effective connectivities (synaptic strengths) or neuronal sensitivity in V1 can be modified. The modification process could mainly target the CS-preferred cells because they are most informative about the CS. These sensitized neurons generate the fear-related signals and propagate the signals to the other neurons via local lateral connections that tend to be nonspecific to orientation [28]. This proposed mechanism can account for the early and specific V1 enhancement associated with the CS. Validation of this speculation requires future causal studies, such as simultaneous recording from the related structures and manipulating neural activities in the amygdala and pulvinar.

STAR★METHODS

Detailed methods are provided in the online version of this paper and include the following:

- KEY RESOURCES TABLE
- LEAD CONTACT AND MATERIALS AVAILABILITY
- EXPERIMENTAL MODEL AND SUBJECT DETAILS
  - Animal preparation
  - Training procedure
- METHOD DETAILS
  - Visual stimuli
  - Data acquisition
- QUANTIFICATION AND STATISTICAL ANALYSIS
  - Mapping RFs and orientation tuning curves
  - Analysis of neuronal responses
  - Latency analysis
- DATA AND CODE AVAILABILITY

SUPPLEMENTAL INFORMATION

Supplemental Information can be found online at https://doi.org/10.1016/j.cub.2019.09.063.

ACKNOWLEDGMENTS

This work was supported by the National Natural Science Foundation of China (91432102 and 31671079), the Interdiscipline Research Funds of Beijing Normal University, and Open Research Fund of the State Key Laboratory of Cognitive Neuroscience and Learning. We thank Xibin Xu and Yin Yan for technical assistance.

AUTHOR CONTRIBUTIONS

Z.L., K.G., and W.L. designed the experiments; Z.L. and A.Y conducted the experiments and analyzed the data; Z.L., K.G., and W.L. wrote the paper.

DECLARATION OF INTERESTS

The authors declare no competing interests.

Received: June 16, 2019
Revised: August 27, 2019
Accepted: September 24, 2019
Published: October 24, 2019

REFERENCES

1. Roelfsema, P.R., and de Lange, F.P. (2016). Early visual cortex as a multiscale cognitive blackboard. Annu. Rev. Vis. Sci. *2*, 131–151.
2. Li, W. (2016). Perceptual learning: Use-dependent cortical plasticity. Annu. Rev. Vis. Sci. *2*, 109–130.
3. Lim, S.-L., Padmala, S., and Pessoa, L. (2009). Segregating the significant from the mundane on a moment-to-moment basis via direct and indirect amygdala contributions. Proc. Natl. Acad. Sci. USA *106*, 16841–16846.
4. Shalev, L., Paz, R., and Avidan, G. (2018). Visual aversive learning compromises sensory discrimination. J. Neurosci. *38*, 2766–2779.
5. Rhodes, L.J., Ruiz, A., Ríos, M., Nguyen, T., and Miskovic, V. (2018). Differential aversive learning enhances orientation discrimination. Cogn. Emotion *32*, 885–891.
6. Stolarova, M., Keil, A., and Moratti, S. (2006). Modulation of the C1 visual event-related component by conditioned stimuli: evidence for sensory plasticity in early affective perception. Cereb. Cortex *16*, 876–887.
7. Keil, A., Stolarova, M., Moratti, S., and Ray, W.J. (2007). Adaptation in human visual cortex as a mechanism for rapid discrimination of aversive stimuli. Neuroimage *36*, 472–479.
8. McTeague, L.M., Gruss, L.F., and Keil, A. (2015). Aversive learning shapes neuronal orientation tuning in human visual cortex. Nat. Commun. *6*, 7823.
9. Thigpen, N.N., Bartsch, F., and Keil, A. (2017). The malleability of emotional perception: Short-term plasticity in retinotopic neurons accompanies the formation of perceptual biases to threat. J. Exp. Psychol. Gen. *146*, 464–471.
10. Paton, J.J., Belova, M.A., Morrison, S.E., and Salzman, C.D. (2006). The primate amygdala represents the positive and negative value of visual stimuli during learning. Nature *439*, 865–870.
11. Buffalo, E.A., Fries, P., Landman, R., Liang, H., and Desimone, R. (2010). A backward progression of attentional effects in the ventral stream. Proc. Natl. Acad. Sci. USA *107*, 361–365.
12. Stănişor, L., van der Togt, C., Pennartz, C.M.A., and Roelfsema, P.R. (2013). A unified selection signal for attention and reward in primary visual cortex. Proc. Natl. Acad. Sci. USA *110*, 9136–9141.
13. Belova, M.A., Paton, J.J., and Salzman, C.D. (2008). Moment-to-moment tracking of state value in the amygdala. J. Neurosci. *28*, 10023–10030.
14. Gothard, K.M., Battaglia, F.P., Erickson, C.A., Spitler, K.M., and Amaral, D.G. (2007). Neural responses to facial expression and face identity in the monkey amygdala. J. Neurophysiol. *97*, 1671–1683.
15. Peck, C.J., Lau, B., and Salzman, C.D. (2013). The primate amygdala combines information about space and value. Nat. Neurosci. *16*, 340–348.
16. Saez, A., Rigotti, M., Ostojic, S., Fusi, S., and Salzman, C.D. (2015). Abstract context representations in primate amygdala and prefrontal cortex. Neuron *87*, 869–881.

17. Schoups, A., Vogels, R., Qian, N., and Orban, G. (2001). Practising orientation identification improves orientation coding in V1 neurons. Nature *412*, 549–553.

18. Yan, Y., Rasch, M.J., Chen, M., Xiang, X., Huang, M., Wu, S., and Li, W. (2014). Perceptual training continuously refines neuronal population codes in primary visual cortex. Nat. Neurosci. *17*, 1380–1387.

19. Yan, Y., Zhaoping, L., and Li, W. (2018). Bottom-up saliency and top-down learning in the primary visual cortex of monkeys. Proc. Natl. Acad. Sci. USA *115*, 10499–10504.

20. Roelfsema, P.R., van Ooyen, A., and Watanabe, T. (2010). Perceptual learning rules based on reinforcers and attention. Trends Cogn. Sci. *14*, 64–71.

21. Janak, P.H., and Tye, K.M. (2015). From circuits to behaviour in the amygdala. Nature *517*, 284–292.

22. Amaral, D.G., Behniea, H., and Kelly, J.L. (2003). Topographic organization of projections from the amygdala to the visual cortex in the macaque monkey. Neuroscience *118*, 1099–1120.

23. Freese, J.L., and Amaral, D.G. (2005). The organization of projections from the amygdala to visual cortical areas TE and V1 in the macaque monkey. J. Comp. Neurol. *486*, 295–317.

24. Pessoa, L., and Adolphs, R. (2010). Emotion processing and the amygdala: from a 'low road' to 'many roads' of evaluating biological significance. Nat. Rev. Neurosci. *11*, 773–783.

25. Bridge, H., Leopold, D.A., and Bourne, J.A. (2016). Adaptive pulvinar circuitry supports visual cognition. Trends Cogn. Sci. *20*, 146–157.

26. Purushothaman, G., Marion, R., Li, K., and Casagrande, V.A. (2012). Gating and control of primary visual cortex by pulvinar. Nat. Neurosci. *15*, 905–912.

27. Zhou, H., Schafer, R.J., and Desimone, R. (2016). Pulvinar-cortex interactions in vision and attention. Neuron *89*, 209–220.

28. Stettler, D.D., Das, A., Bennett, J., and Gilbert, C.D. (2002). Lateral connectivity and contextual interactions in macaque primary visual cortex. Neuron *36*, 739–750.

29. Khayat, P.S., Pooresmaeili, A., and Roelfsema, P.R. (2009). Time course of attentional modulation in the frontal eye field during curve tracing. J. Neurophysiol. *101*, 1813–1822.

STAR★METHODS

KEY RESOURCES TABLE

REAGENT or RESOURCE	SOURCE	IDENTIFIER
Experimental Models: Organisms/Strains		
Rhesus monkeys (*Macaca mulatta*)	Beijing Prima Biotech Inc.	http://www.primasbio.com/en/Home
Software and Algorithms		
MATLAB 2018b	MathWorks	https://www.mathworks.com
Other		
Cerebus System (128 channels)	Blackrock Microsystems	PN# 4176
Utah Array (96 channels)	Blackrock Microsystems	SN# 4566-001277 SN# 4566-001303

LEAD CONTACT AND MATERIALS AVAILABILITY

This study did not generate new unique reagents. Further information and requests for resources should be directed to and will be fulfilled by the Lead Contact, Wu Li (liwu@bnu.edu.cn).

EXPERIMENTAL MODEL AND SUBJECT DETAILS

Animal preparation

All experimental procedures complied with the US National Institutes of Health Guide for the Care and Use of Laboratory Animals and were also approved by the Institutional Animal Care and Use Committee of Beijing Normal University.

Two adult monkeys (*Macaca mulatta*, male, 7-9 Kg; named MA and MB) were used. Each animal underwent two surgical operations under anesthesia (1.5%–2.5% isoflurane) in an aseptic environment: one for attaching a titanium post to the skull with bone screws; the other for implanting microelectrode arrays in V1 (two 6 × 8 arrays, 0.5 mm long electrodes with 0.4 mm inter-electrode spacing; Blackrock Microsystems, USA).

Training procedure

The monkeys, with the head fixed using the implanted post, were first trained to do a fixation task, in which they were required to maintain fixation at a small point in exchange for a drop of juice. They were then trained to differentiate between gratings tilted to the right and left relative to the vertical. Afterward, the animals were trained using the fear conditioning paradigm described in the main text (Figure 1A).

METHOD DETAILS

Visual stimuli

Visual stimuli were generated by a stimulus generator (ViSaGe MKII; Cambridge Research Systems) on a gamma-corrected CRT monitor (Iiyama Pro-513; 1,200 × 900 pixels at 100 Hz, maximal luminance 40.6 cd/m^2, 100-cm viewing distance). All the stimuli were displayed on a gray background of 20.3 cd/m^2.

The visual stimuli used in the conditioning experiments were square-wave (Figures 1, 2, and 4) or sine-wave (Figure 3) drifting gratings (4° in diameter, 2 cycles/degree, drifting at 2 cycles/s, 100% contrast). The orientations of gratings were set as indicated in the main text.

Data acquisition

Neuronal spiking activities in V1 were recorded by the implanted microelectrode arrays using a 128-channel data acquisition system (Blackrock Microsystems, USA). The raw data were high-pass filtered (4th order Butterworth with 250 Hz corner frequency). Multi-unit activities were detected by applying a voltage threshold at a signal-to-noise ratio of 4-4.5. Spike waveforms were digitized and recorded at 30 kHz.

During a trial in the conditioning sessions or pre- and post-tests, eye positions were measured by an infrared eye tracker (EyeLink 1000, SR Research Ltd., Canada) at 500 Hz sampling rate. Before the offset of grating stimuli, the animal was required to maintain its fixation within an invisible window (0.75° in radius) centered on the fixation spot (0.12° in diameter). During the trace interval of a conditioning trial, eye blinks or closures were detected by the eye tracker.

QUANTIFICATION AND STATISTICAL ANALYSIS

Mapping RFs and orientation tuning curves

Before daily experiments, V1 neurons' RFs and orientation tuning curves were determined using square-wave drifting gratings. By placing a grating patch elongated vertically (0.3° × 6°) or horizontally (6° × 0.3°) at different locations along the horizontal or vertical axis, we collected the spiking activities from each electrode (referred to as a V1 site). Mean neuronal responses as a function of the stimulus locations were fitted with a Gaussian. The RF center was measured as the Gaussian center, and the RF size along either dimension was defined as 1.96 SD of the Gaussian. To determine the orientation tuning curve and the preferred orientation for each site, we set a 5°-diameter grating patch at different orientations and drifting directions (−180° to 180°, 15° step). The preferred orientation for each recording site was determined by Gaussian fit. The goodness of fit was estimated using R^2; only recording sites with $R^2 > 0.7$ in both the RF profiles and orientation tuning were included in further data analysis. The number of contributing electrodes slightly varied between days due to changes in signal quality.

Analysis of neuronal responses

We treated responses recorded by the same electrode in different days as coming from the same sample (a single V1 site). The population averaged peri-stimulus time histograms (PSTHs, Figures 1C, 2C, 2D, and 3C) were made by the follow steps: binning the spikes into 1-ms bins for each trial and each site; averaging the binned spike counts across trials for each site and smoothing the resulting raw PSTH with a 10-ms moving square window; and averaging the smoothed PSTHs from all sites.

The mean spontaneous activity was calculated using 200-ms period before the onset of gratings. To measure the fear-related signals for each V1 site, we first calculated the mean neuronal responses within 30-70 ms after stimulus onset in the conditioning trials and pre-test trials, with the respective mean spontaneous activity subtracted on a trial-by-trial basis. We used the Mann-Whitney U test to examine whether the mean neuronal response in the conditioning sessions was significantly larger than that in the pre-tests within the 30-70 ms window. Those V1 sites with $p < 0.05$ were defined as significant sites.

Latency analysis

The latencies of V1 responses evoked by the CS or NS were measured from the population-averaged PSTH after subtracting the mean spontaneous activity and fitting the PSTH with the following function [29]:

$$f(t) = d \times exp\left(\mu\alpha + 0.5\sigma^2\alpha^2 - \alpha t\right) \times G\left(t, \mu + \sigma^2\alpha, \sigma\right) + c \times G(t, \mu, \sigma)$$

$G(t, \mu, \sigma)$ is a cumulative Gaussian. The visual response latency was defined as the time point when the fitted curve reached 33% of its maximum. The latency of fear-related signals was calculated in a similar way based on the differential PSTH between the conditioning sessions and pre-tests.

We computed the mean and SD of the latency through resampling: For a total of *n* recorded V1 sites, we randomly drew, with replacement, *n* sites from the dataset and calculated the latency using the population-averaged PSTH. The mean and SD were estimated after repeating this procedure 1,000 times.

DATA AND CODE AVAILABILITY

The raw datasets and code supporting the current study have not been deposited in a public repository because the neural and behavioral data were stored in self-customized and rather complicated binary format (there is no standardized format for storing and sharing data in electrophysiological studies on behaving monkeys); but the data are available from the corresponding author upon specific request.